

The synthesis and characterization of undoped and Ni doped CeO₂ nanoparticles using sol-gel method

V. Ramasamy^{1*}, V. Mohana¹ and G. Suresh²

¹*Department of Physics, Annamalai University, Annamalai Nagar, 608 002, India*

²*Department of Physics (DDE-WING), Annamalai University, Annamalai Nagar, 608 002, India*

**E-mail: srsaranram@rediffmail.com*

ABSTRACT

Undoped and Ni doped CeO₂ nanoparticles were synthesized using sol-gel technique with varying Ni dopant concentrations. The obtained products were characterized by X-ray diffraction (XRD), UV-Vis absorption and scanning electron microscopy with energy dispersive X-ray analysis (SEM-EDX). The XRD measurements indicate that the nanoparticles have cubic structured CeO₂ crystallites. The calculated average crystallite sizes varied from 10.98 to 35.43nm. SEM-EDAX analysis shows the morphology and the presence of elements in the sample. The optical properties of the nanoparticles are observed by UV- visible spectroscopy. The effect of dopant with observed band shift is due to quantum confinement effect.

Keywords: Nanoparticles, sol-gel technique, cubic structure, optical properties, quantum confinement effect.

Introduction

Ceria or cerium oxide exist as natural mineral (called as cerianite) that has been identified as a secondary mineral at the many localities worldwide, including weathered phonolites and nepheline syenites, hydrothermal veins, granite pegmatite, alluvial deposits, alkaline pegmatite, etc., [1]. Cerium is a lanthanide series rare earth element, and is the most abundant of these rare earths, present at about 66 ppm in the earth's crust [2]. It is found in a number of minerals such as bastnäsite, monazite, gadolinite, fergusonite, samarskite, xenotime, yttrocerite, cerite allanite (or orthite), etc. Conversely, synthetic cerium oxide (CeO_2) having cubic structure is the most important oxide related to its extraordinary chemical properties (acidebase and oxidation-reduction behavior), thermal stability and oxygen mobility [1]. Cerium can also exist in either the free metal or oxide form, and can cycle between the cerous, cerium (III), and ceric, cerium (IV), oxidation states [2]. Both oxidation states of cerium strongly absorb ultraviolet light and have two characteristic spectrophotometric absorbance peaks. The first peak is in the 230–260 nm range and corresponds to cerium (III) absorbance. The second peak absorbance occurs in the 300–400 nm range and corresponds to cerium (IV) absorbance [3]. Over the past decade, cerium oxide nanoparticles (CeO_2 nanoparticles) have been widely studied for their structural, chemical, and physical properties, such as non-stoichiometry, reduction behavior, oxygen storage capacity and interactions of metal/ CeO_2 nanoparticles [4-6]. CeO_2 nanoparticles have also shown several other technologically important applications including fuel cells [7], catalyst [8], sun screen cosmetics [9], sensor [10] and UV blockers [11]. Generally, CeO_2 nanoparticles were synthesized by physical and chemical methods such as precipitation, sol-gel, spray drying system, thermal decomposition and microemulsion procedure. The sol-gel method has become very popular due to its versatility, better purity, low processing temperature, and the possibility of controlling the size and morphology of grains.

In the present work, undoped and Ni doped CeO_2 nanoparticles were synthesized by sol-gel method. The synthesized nanoparticles were characterized using X-ray diffraction (XRD), Scanning electron microscopy with energy dispersive X-ray analysis (SEM-EDX) and Ultraviolet Visible spectroscopy (UV-Vis).

EXPERIMENTAL TECHNIQUES

Materials

To synthesize undoped and Ni-doped CeO₂ nanoparticles, the following materials were used. Cerium (IV) nitrate (NH₄)₂[Ce(NO₃)₆] obtained from Nice Chemical company, Nickel acetate extra pure (Tetrahydrate) (CH₃.COO)₂Ni.4H₂O obtained from Loba chemie PVT. LTD. Ammonium hydroxide (NH₃) obtained from spectrum reagents and chemicals Pvt. Ltd, Citric acid anhydrous (C₆H₈O₇) obtained from s-d Fine Chem. Ltd, and deionized water (DI). All the chemicals were above 99% purity. Ultrapure water was used for all dilution and sample preparation. Acid washed glass wares used in this experimental work.

Methods

The Ni-doped CeO₂ nanoparticles were synthesized by the sol-gel method. In a typical procedure, 5.2g (0.4M) of Cerium (IV) nitrate (NH₄)₂[Ce(NO₃)₆] in 25ml of deionized water aqueous mixed with Nickel acetate (0.1, 0.3, 0.5 and 0.7 M.%) in 25ml of deionized water under constant stirring. Two solutions were mixed together, and the saturated solution of citric acid was added drop wise in to the mixture. Then, NH₃ was added to the precursor solution in order to maintain same the pH of the solution. After continuous stirring for 4 hours at 70°C, the clear solution was completely turned to a gel. Then, the gel was dried and ground into powder. The powder was calcined at 400°C for 2 hrs in furnace under an air atmosphere using furnace. The same procedure was followed for the synthesis of undoped CeO₂ nanoparticles without adding doping materials.

Characterization of sol-gel derived CeO₂ nanoparticles

The using X pert PRO diffractometer with a Cu K α radiation ($K\alpha = 1.5406 \text{ \AA}$), the X-ray diffraction (XRD) patterns of the powder samples were recorded. The morphological studies of the products were analyzed using scanning electron microscopy. These measurements were performed on a JEOL- 6610 scanning electron microscope. Energy-dispersive X-ray analysis (EDX) measurement was carried out using Brucker 129 eV, to get elemental composition (%). Before the measurement, the samples were mounted on copper stubs by double sided carbon tapes

and the gold is coated using the sputtering technique. The optical absorption spectra of the samples were recorded by UV-1650 PC SHIMADZU spectrometer.

Results and discussion

X-ray diffraction

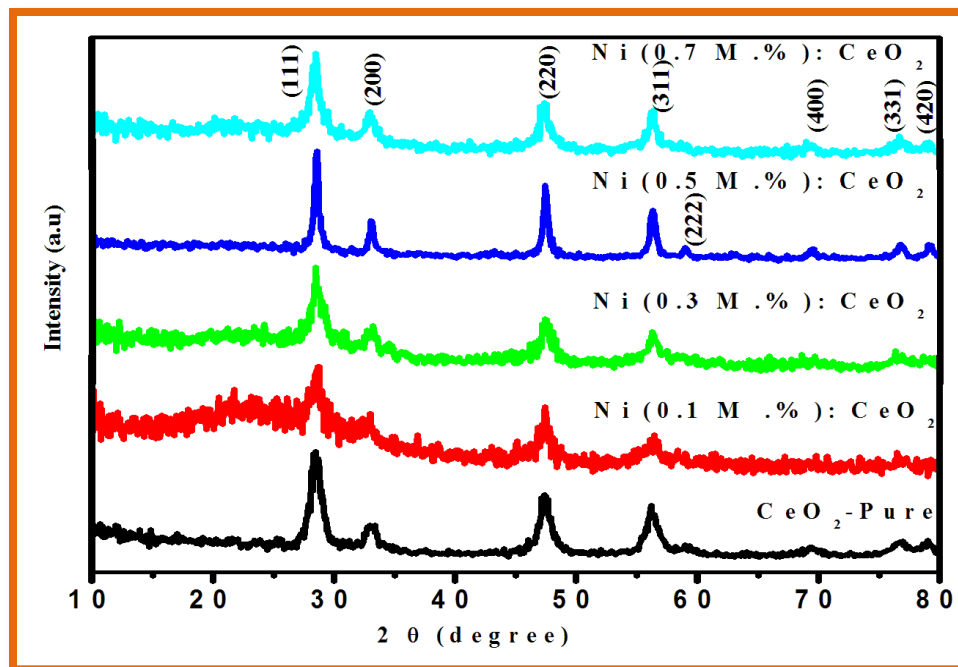


Fig. 1 X-ray diffraction patterns of undoped and Ni doped CeO₂ nanoparticles

The crystal structure and phase identification of the samples were analyzed from the X-ray diffraction patterns. The typical X-ray diffraction patterns of undoped and Ni (0.1, 0.3, 0.5 and 0.7 M.%) doped CeO₂ nanoparticles are shown in Fig 1. The peaks located at an angles (2θ) of 28.51°, 33.03°, 47.42°, 56.24°, 59.08°, 69.35°, 76.72° and 79.12° are attributed to (111), (200), (220), (311), (222), (400), (331) and (420) planes respectively. All the peaks in the pattern were indexed for cubic structure and the lattice constant calculated from XRD data are in closely agreement with the JCPDS (card no: 34-394) [12]. It is noticed that the remarkable features in the XRD of the Ni (0.1 M.%) doped samples are the decrease of peak intensity and increase in the full width at half maximum (FWHM), which suggest that the crystallite size decreases [13].

The average nanocrystalline size is calculated using Debye– Scherrer's formula [14] by following equation (1)

$$D = \frac{K\lambda}{\beta \cos\theta} \quad (1)$$

Where D is the crystallite size, β is the full-width of half maximum (FWHM), K is a shape factor (K=0.9 in this work) and λ is the wavelength of incident X-rays ($\lambda = 0.15406$ nm). The crystallite sizes of the undoped and Ni doped CeO₂ nanoparticles are ranged between 10.98 to 35.43 nm. The crystalline size increases with increasing of Ni concentration. The lower crystalline size (13.58 nm) is observed in 0.1 M.% of Ni doping ceria. This is due to quantum confinement effect.

Scanning electron microscopy (SEM with EDX)

The morphology of the undoped and Ni-doped CeO₂ nanoparticles have been characterized by SEM with EDX analysis. The low and high magnification of different concentration of Ni (0.1, 0.3, 0.5 and 0.7 M.%) doped CeO₂ nanoparticles are shown in Fig. 2 (a-b). The SEM images of 0.1 M.% of Ni doped ceria nanoparticles show large particles which are composed of small crystallites and the particles of aggregates with irregular shapes. The surface morphology of the samples is not clear due to smaller particle size. Fig. 2c shows the energy dispersive X-ray (EDX) spectrum, confirms the presence of Ce, O and Ni.

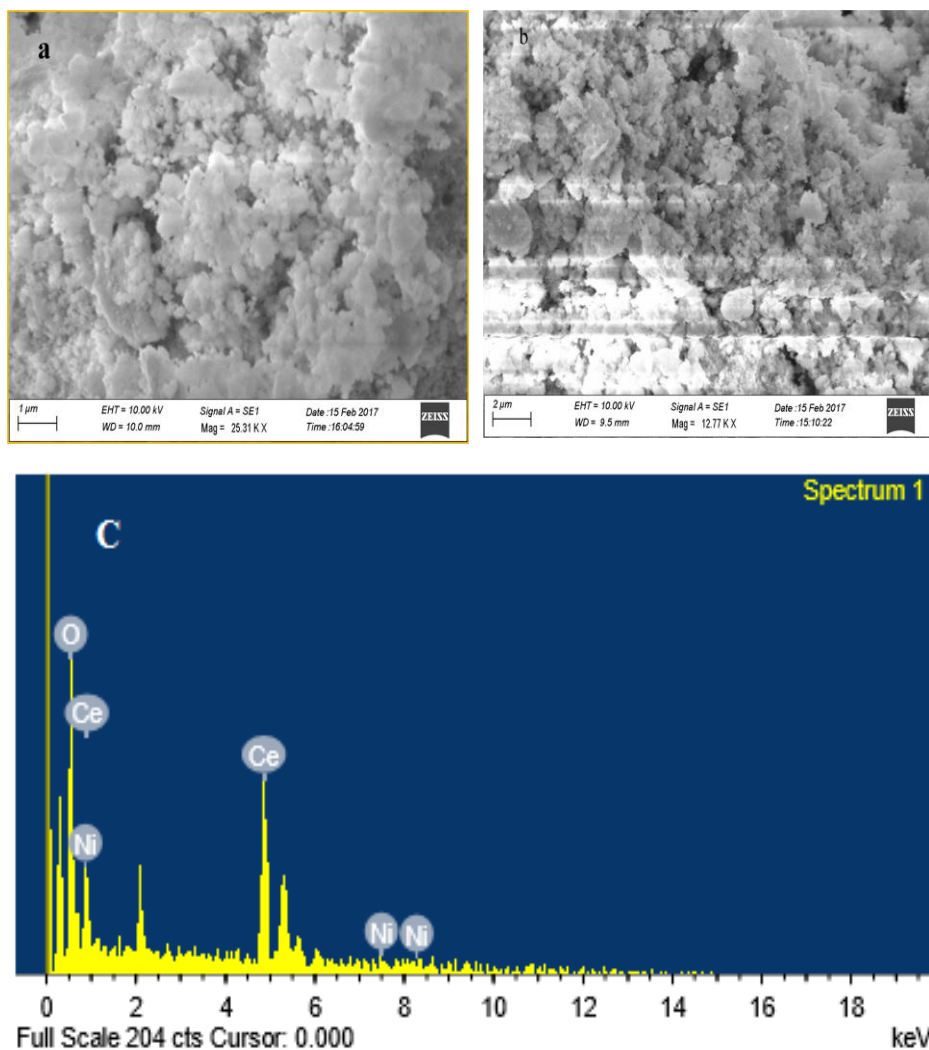


Fig. 2 (a-c) SEM-EDX images of undoped and Ni (0.1 M.%) doped CeO₂ nanoparticles

UV-Visible Spectra

Fig. 3 shows the UV-Vis absorption spectrum of undoped and Ni doped cerium oxide. The spectra exhibit a absorption band between 300-400 nm. The UV- Vis absorption peaks indicate the band gap of particles. The fundamental absorption of the nanoparticles, which corresponds to electron excitation from the valance band to conduction band, was calculated to determine the optical band gap.

The optical band gap energy of the nanoparticles was calculated based on the absorption spectrum of the nanoparticles using Eq. (2).

$$E_g = \frac{1240}{\lambda} \text{ eV} \quad (2)$$

Where, E_g is the optical band gap, and λ is the absorption maximum [15]. The absorption maximum for undoped and Ni (0.1, 0.3, 0.5 and 0.7 M.%) doped CeO_2 nanoparticles are observed in Fig. 3.

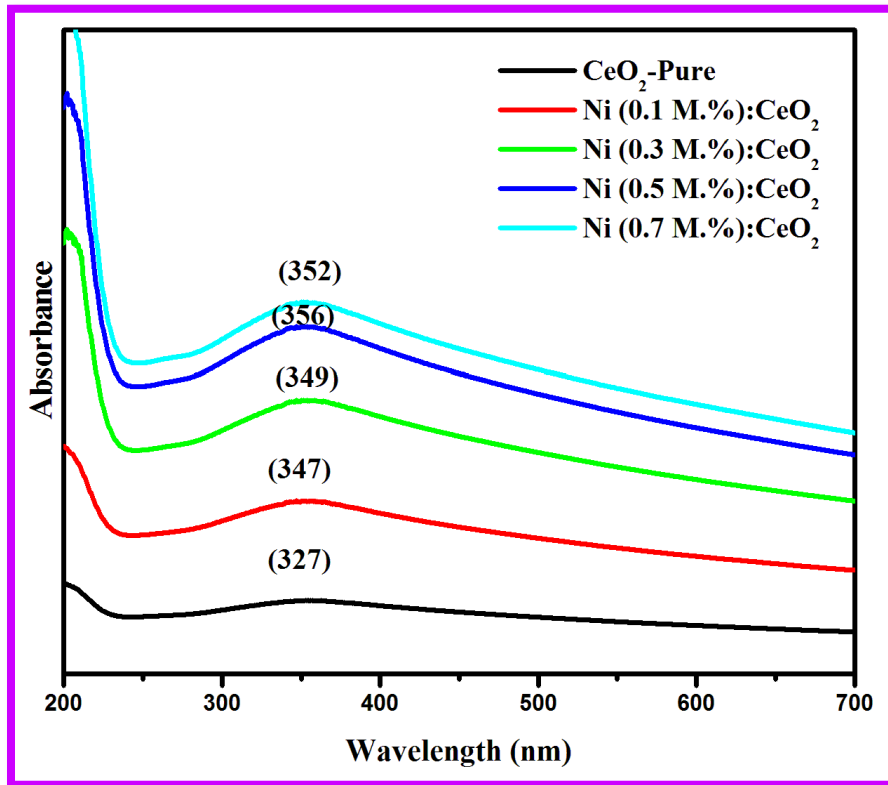


Fig. 3 UV-visible absorption spectrum of undoped and Ni (0.1, 0.3, 0.5 and 0.7 M.%) doped CeO_2 nanoparticles

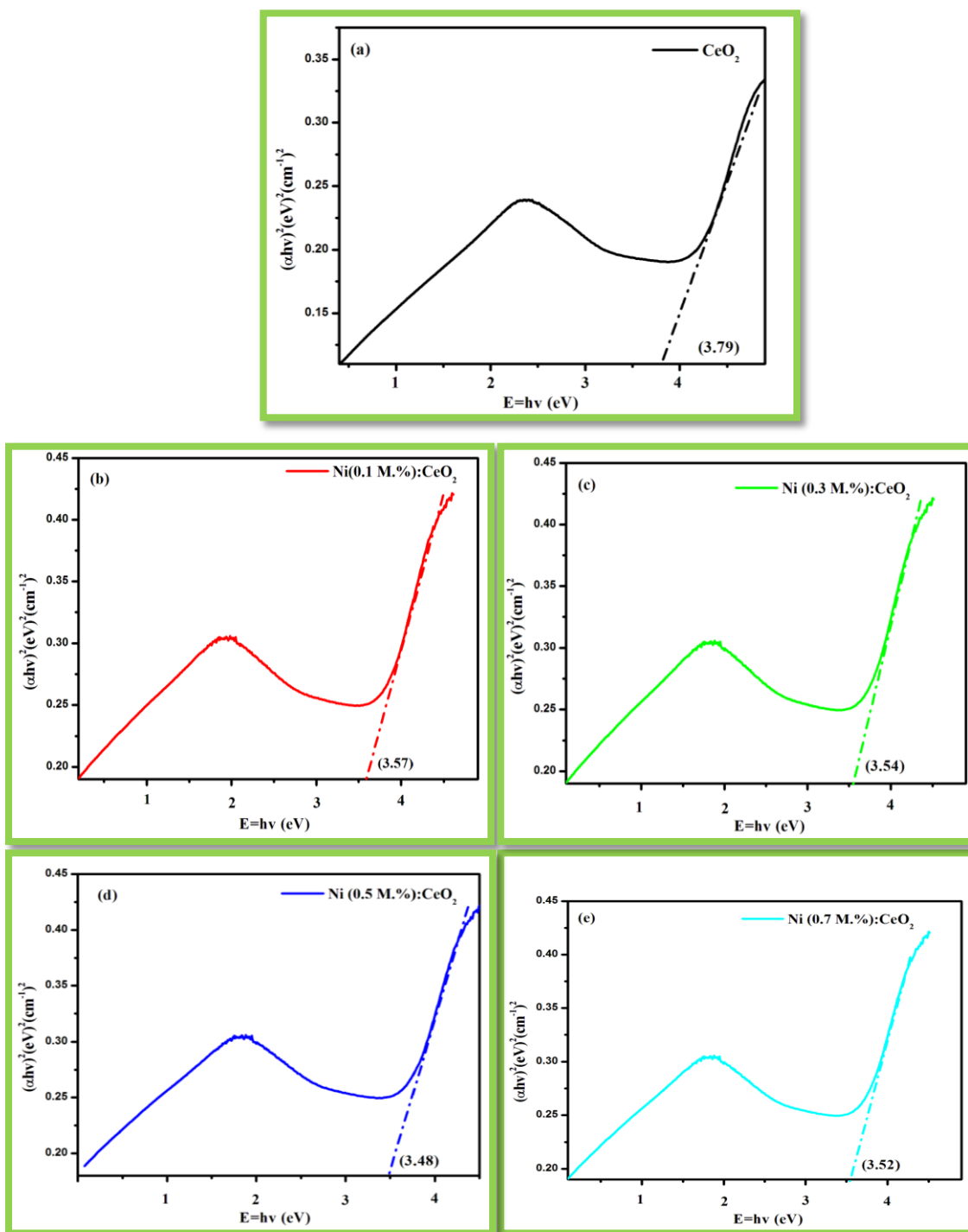


Fig. 4 Optical band gap graphs for Ni (0.1, 0.3, 0.5 and 0.7 M.%) doped Ceria nanoparticles by Tauc plot method

The absorption coefficient α was calculated from the absorption spectra using the following equation (3).

$$\alpha = \frac{2.303 \times 10^3 A \rho}{Lc} \quad (3)$$

Where A is the absorbance, ρ is the real density of CeO₂ (set at 7.28 g cm⁻³ for this calculations), L is the length of the curve, and C is the concentration of the CeO₂ suspension [16]. The band gap corresponding to direct transition is calculated by extrapolating the linear portions of $(\alpha h\nu)^2$ as a function photon energy $h\nu$ for the doped and undoped nanoparticles which are shown in Fig. 4 (a-e).

From these figures the band gap energy values are observed 3.79, 3.57, 3.54, 3.48 and 3.52 eV for undoped and Ni doped samples. However, the band gap values of undoped and doped CeO₂ nanoparticles are higher than that of bulk value (3.19 eV) [17]. The results reveal that the increase of band gap energy increase shows that particle size is reduced. This blue shift in absorption spectra is attributed to the quantum confinement effect [18].

Conclusion

The undoped and Ni doped CeO₂ nanoparticles have been successfully synthesized by sol-gel method. The XRD patterns showed that the materials were in nanometer regime with cubic structure. The size of as prepared particles is found to be in 10.98 to 35.43 nm range. SEM images conformed that Ni (0.1 M.%) doped CeO₂ nanoparticles have better distributed particles and also synthesized nanoparticles via sol-gel method had the smallest particle size. The blue shift of Ni doped CeO₂ dictates the quantum confinement effect. The band gap energy has observed by UV-visible which is highly greater than that of undoped, bulk, and other reported values.

Reference:

- [1]. G. Montes-Hernandez, R. Chiriac, N. Findling, F. Toche, and F. Renard “Synthesis of ceria (CeO_2 and CeO_{2-x}) nanoparticles via decarbonation and Ce(III) oxydation of synthetic bastnäsite (CeCO_3F),” *Materials Chemistry and Physics*, 172, (2016), pp. 202–210.
- [2]. Z. Hu, S. Haneklaus, G. Sparovek, and E. Schnug, “Rare Earth Elements in Soils,” *Communications in Soil Science and Plant Analysis*, 37, 9–10, (2006), pp. 1381–1420.
- [3]. A. Medalia and B. Byrne, Spectrophotometric Determination of of Cerium (IV),” *Analytical Chemistry*, 23, 3, (1951), pp. 453–456.
- [4]. M. Darroudi, M. Hakimi, M. Sarani, R. Kazemi Oskuee, A. Khorsand Zak, and L. Gholami, “Facile synthesis, characterization, and evaluation of neurotoxicity effect of cerium oxide nanoparticles,” *Ceramics International*, 39, 6, (2013), pp. 6917–6921.
- [5]. R.B. Duarte, M. Nachtegaal, J.M.C. Bueno, J.A. van Bokhoven, “Understanding the effect of Sm_2O_3 and CeO_2 promoters on the structure and activity of $\text{Rh}/\text{Al}_2\text{O}_3$ catalysts in methane steam reforming,” *Journal of Catalysis*, 296, (2012), pp. 86–98.
- [6]. V.B. Mortola, S. Damyanova, D. Zanchet, J.M.C. Bueno, “Surface and structural features of $\text{Pt}/\text{CeO}_2\text{-La}_2\text{O}_3\text{-Al}_2\text{O}_3$ catalysts for partial oxidation and steam reforming of methane,” *Appl. Catal. B: Environ*, 107, (2011), pp. 221–236.
- [7]. A. B. Stambouli and E. Traversa, “Solid oxide fuel cells (SOFCs): a review of an environmentally clean and efficient source of energy,” *Renewable and Sustainable Energy Reviews*, 6, 5, (2002), pp. 433–455.
- [8]. E. Bekyarova, P. Fornasiero, J. Kašpar, and M. Graziani, “CO oxidation on $\text{Pd}/\text{CeO}_2\text{-ZrO}_2$ catalysts,” *Catalysis Today*, 45, 1–4, (1998), pp. 179–183.
- [9]. S. Yabe, “Cerium oxide for sunscreen cosmetics,” *Journal of Solid State Chemistry*, 171, 1–2, (2003), pp. 7–11.
- [10]. S. B. Khan, M. Faisal, M. M. Rahman, and A. Jamal, “Exploration of CeO_2 nanoparticles as a chemi-sensor and photo-catalyst for environmental applications,” *The Total Environment*, vol. 409, 15, (2011), pp. 2987–2992.
- [11]. S. D. Senanayake, D. Stacchiola, and J. A. Rodriguez, “Unique Properties of Ceria Nanoparticles Supported on Metals: Novel Inverse Ceria/Copper Catalysts for CO Oxidation and the Water-Gas Shift Reaction,” *Accounts of Chemical Research*, 46, 8, (2013), pp. 1702–1711.
- [12]. J. Zhang, H. Yang, S. Wang, W. Liu, X. Liu, J. Guo, and Y. Yang, “Mesoporous CeO_2 nanoparticles assembled by hollow nanostructures: formation mechanism and enhanced catalytic properties,” *Cryst Eng Comm*, 16, 37, (2014), p. 8777.
- [13]. X. Yang, X. Yu, and G. Li, “The effects of Nd doping on the morphology and optical properties of CeO_2 nanorods,” *Journal of Materials Science: Materials in Electronics*, 27, 9, (2016), pp. 9704–9709.
- [14]. P. Scherrer and *Göttinger Nachrichten*, 2 (1918), p 98.
- [15]. E. D. Sherly, J. J. Vijaya, and L. J. Kennedy, “Effect of CeO_2 coupling on the structural, optical and photocatalytic properties of ZnO nanoparticle,” *Journal of Molecular Structure*, 1099, (2015), pp. 114–125.
- [16]. F. Cheviré, F. Muñoz, C. F. Baker, F. Tessier, O. Larcher, S. Boujday, C. Colbeau-Justin, and R. Marchand, “UV absorption properties of ceria-modified compositions within the fluorite-type solid solution $\text{CeO}_2\text{-Y}_6\text{WO}_{12}$,” *Journal of Solid State Chemistry*, 179, 10, (2006), pp. 3184–3190.
- [17]. E. Moghaddam, A.A. Youzbashi, A. Kazemzadeh, M.J. Eshraghi, “Preparation of surface-modified ZnO quantum dots through an ultrasound assisted sol–gel process,” *J. Appl. Surf. Sci*, 346, (2015), pp. 111–114.
- [18]. S. Samiee and E. K. Goharshadi, “Effects of different precursors on size and optical properties of ceria nanoparticles prepared by microwave-assisted method,” *Materials Research Bulletin*, 47, 4, (2012), pp. 1089–1095.